Towards decoding the coupling decision-making of epithelial-mesenchymal transition and metabolic reprogramming in cancer

Madeline Galbraith[1], Dongya Jia[2], Herbert Levine[3], and José Onuchic[1]

[1]Center for Theoretical Biological Physics, Rice University, Houston, TX, USA

[2]Immunodynamics Group, Laboratory of Integrative Cancer Immunology, Center for Cancer Research, National Cancer Institute, Bethesda, MD, USA

[3]Center for Theoretical Biological Physics, Department of Physics, and Department of Bioengineering, Northeastern University, Boston, MA, USA

Abstract

Abnormal metabolism and attaining motility are two hallmarks of cancer. During metastasis, a developmental program, epithelial-mesenchymal transition (EMT) is often used by cancer cells to become motile. Aside from complete EMT, cancer cells can alternatively acquire a hybrid epithelial/mesenchymal (E/M) phenotype, which combines the features of E and M, and in many cases serves as the primary instigator of metastasis. Cancer cells have been observed to largely use glycolysis irrespective of the presence of oxygen, referred to as the Warburg effect (W). In addition to glycolysis, when leaving the primary tumor and entering blood circulation, cancer cells can increase their mitochondrial oxidative phosphorylation (OXPHOS, O) without compromising their glycolytic activity, thus entering a hybrid metabolic mode (W/O). The W/O state has often been observed to be associated with enhanced metastatic potentials. Understanding the relationship between cancer metabolism and EMT can therefore offer novel anti-metastasis strategies. Here, we analyze the relationship between metabolism and EMT by coupling their corresponding core decision-making molecular networks – AMPK/HIF-1/ROS and μ_{34}/SNAIL/μ_{200}/ZEB, respectively. We systematically elucidate how different phenotypes

during EMT (E, M and hybrid E/M) are associated with different metabolic phenotypes (O, W and W/O). Specifically, we identified the feedback loops that lead to the coupling of the E/M state with the W/O state, referred to as E/M-W/O, a potentially highly aggressive phenotype. Strikingly, we found that even if the individual molecular network of EMT or metabolism does not support a hybrid phenotype, the crosstalk can give rise to the E/M-W/O state. Moreover, in this case, there is an order of events in that the W/O state emerges first and is followed by the E/M state, suggesting that metabolic reprogramming can be a primary driver of EMT and the acquisition of highly metastatic hybrid E/M cells.

Introduction

Metastasis remains the leading cause of cancer-related deaths [1] and thus it is critical to understand the physiological properties of cells that migrate from the primary tumor and initiate metastatic lesions. Typically, these properties have been studied one at a time. For example, cell motility is assumed to be related to the epithelial-mesenchymal transition (EMT). During EMT, the cells progressively lose epithelial (E) features such as cell-cell adhesion and apical-basal polarity, and acquire mesenchymal (M) features such as migration, invasion, and resistance to immune response [2,3]. The EMT has consistently been implicated in cells acquiring metastatic potential [4,5], and also plays a role in therapeutic resistance [6]. Recently, the bimodal picture of EMT has been superseded by a more complex scenario involving the hybrid epithelial/mesenchymal (E/M) phenotype which exhibits combined traits of epithelial (cell-cell adhesion) and mesenchymal (invasion) at the single-cell level. The hybrid E/M cells migrate collectively as a cluster and may account for the majority of metastases [7–10]. The existence of a hybrid E/M state has since been experimentally verified both in vitro (in many cancer cell lines) and in vivo (e.g. using a genetic mouse model of squamous cell carcinoma) and has been

shown to be associated with therapy resistance alongside with poor survival rates [11–14]. Most importantly, these states appear to the most capable of initiating metastatic growth [15,16]. Fully understanding the behavior of the hybrid E/M phenotype is still an active area of research.

Metabolic reprogramming, another hallmark of cancer, enables cancer cells to adjust their metabolic activity for biomass and energy supply to survive in hostile environments [1,17]. Normal cells typically utilize oxidative phosphorylation (OXPHOS, O) under normoxic conditions and glycolysis when there is a lack of oxygen. However, cancer cells often prefer glycolysis even when oxygen is available, referred to as the Warburg effect (W) or aerobic glycolysis [18,19]. During metastasis, cancer cells must be able to adjust their metabolic phenotype in order to survive in varying environments, resulting in these cells switching between different types of metabolism [20–23]. Metabolic reprogramming, specifically in the context of switching between the O state and W state, can enable cancer cells to combine different metabolic modes, leading to the acquisition of a hybrid W/O phenotype and metabolic low-low phenotype (L/L). The W/O cells, often associated with enhanced metabolic potentials, actively use both glycolysis and OXPHOS [24,25]. The L/L cells are metabolically inactive, exhibiting both low glycolysis and low OXPHOS, and are associated with therapy resistance in melanoma [26]. The highly metastatic murine breast cancer 4T1 cells exhibit both higher glycolytic and OXPHOS activity relative to the isogenic and less metastatic 67NR cells [27]. Furthermore, when the circulating tumor cells (CTCs) formed by 4T-1 cells exhibited enhanced OXPHOS relative to both the primary tumor and lung metastasis formed by 4T1 [28]. The high metastatic potential enabled by the hybrid metabolic phenotype has been confirmed in a number of additional experimental studies [27,29]. Together, these experiments suggest a tight connection

between metabolic plasticity and cancer metastasis, specifically the hybrid W/O state with high metastatic potential.

As already mentioned, many studies focused on either EMT or metabolism[7–10,20–23]. However, it has become increasingly clear that there exists extensive crosstalk between EMT and metabolism [29]. For example, there is bi-directional regulation between hypoxia-inducible factor 1 (HIF-1) and miR-200 [30]. The repression of miR-200 by HIF-1 induces EMT [31] and HIF-1 is able to repress the expression of HIF-1 [32]. Understanding the crosstalk between EMT and metabolic reprogramming is important for an increased comprehension of metastasis and tumor proliferation [29,33–35]. Recent studies show that metabolic reprogramming can increase metastatic potential and drive EMT, or conversely that induction of EMT can drive metabolic reprogramming [36–39]. The underlying mechanisms of interaction between EMT and metabolic reprogramming remain poorly understood, with several competing hypotheses as discussed below. Kang et. al. suggested cancer cells typically undergo metabolic reprogramming first and then trigger EMT [40,41]; this coupling, presumably, is a consequence of changes in the tumor microenvironment fostering metabolic reprogramming which drives EMT [42–44]. Another hypothesis is that the mutual activation between EMT and metabolic reprogramming can contribute to flexible coupling of various EMT states (E, M, and E/M) with different metabolic states (W, O, W/O) and possibly the two hybrid phenotypes (E/M and W/O) become coupled under certain crosstalk, leading to a greatly increased metastatic potential [29]. Evidence supporting this connection has recently been noticed in CTCs, where the CTCs exhibit enhanced OXPHOS with no compromise in glycolysis [28] and have also been shown to mainly consist of hybrid E/M cells, especially at high levels of NRF2, an antioxidation regulator [45]. Consistent coupling of E/M and W/O has been seen in breast cancer stem cells (BCSCs). Specifically, the

hybrid E/M-like BCSCs (E/M-BCSCs) exhibit higher levels of both OXPHOS and glycolysis as compared to the mesenchymal-like BCSCs (M-BCSCs) [46,47]. While there have been preliminary indications of the coupling of EMT states and metabolic states, a systematic analysis of how different EMT and metabolism states are coupled remains to be explored.

To decode the coupled decision-making of EMT and metabolism, we developed a mathematical model which couples the core gene regulatory circuit of EMT – μ_{34}/SNAIL/μ_{200}/ZEB [7] with that of metabolism – AMPK/HIF-1/ROS [48]. Regarding the EMT circuit, the miRNAs, μ_{34} and μ_{200} promote the E state while the transcription factors (TFs) SNAIL and ZEB promote the M state. In the metabolism circuit, AMPK promotes the O state while HIF-1 promotes the W state, and the reactive oxygen species (ROS) may be associated with the W/O state. By analyzing the coupled circuit, we found that mtROS is a key promoter of "double-hybrid" state, namely the hybrid E/M state coupled with the hybrid metabolic phenotype, referred to as the E/M-W/O state. Additionally, as we will show later, HIF-1 may play a more central role in metabolic reprogramming driving EMT than AMPK. Strikingly, we found that when the crosstalk is bi-directional there are parameter space regions for which the E/M-W/O state is the only accessible state, and the biological significance of these parameters will depend on details of the microenvironment. Interestingly, even if the individual circuit cannot give rise to the hybrid phenotype (i.e., neither the E/M or W/O states are initially accessible), upon including crosstalk, the hybrid states (E/M or W/O) emerge. Indeed, a single crosstalk is sufficient for the metabolism circuit or EMT circuit to gain tristability. We also show that previously identified phenotypic stability factors (PSFs) of the E/M state - GRHL2 and OVOL2 [14,49], not only stabilize the E/M state but also stabilized the E/M-W/O state. Our results therefore suggest that a highly aggressive plastic phenotype along both the EMT and

metabolic axes (E/M-W/O) is a likely choice for a subset of cancer cells and, speculatively, may be critical for metastasis.

Model: Coupling the regulatory networks of EMT and metabolism

While the mechanisms of EMT and cancer metabolism have been investigated individually, the crosstalk between the two circuits and how the phenotypes are correlated is still largely unknown. To decode the crosstalk between EMT and metabolism, we couple our previously published regulatory networks of EMT [7] and metabolism [48] by including the mutual regulatory links between these two circuits; see Fig. 1A for the coupled network and see SI for details for each of the crosstalks (Table S5). The crosstalk between the EMT circuit and the metabolism circuit can be direct (e.g., HIF-1 upregulating SNAIL) or indirect (e.g., μ_{34} upregulating mtROS), the latter arising because our formulation focuses only on a few core components and effective interactions between them that can occur via intermediate reactants. We initially focus on the core networks and investigate the role of crosstalk on the coupling of different EMT and metabolism states. Then we ask an interesting question whether the crosstalks contributed to the emergence of the hybrid states. Lastly, we evaluate the role of the PSFs of E/M, OVOL and GRHL2,on the stability of the E/M-W/O state.

The core EMT network is comprised of the EMT-inducing transcription factors (EMT-TFs), ZEB and SNAIL, and the microRNA families, μ_{200} and μ_{34}. It is modeled as a transcription-translation chimeric circuit [7]. For a two-component chimeric circuit consisting of one microRNA (u) and one TF (RNA m, protein B), the binding/unbinding dynamics are given by

$$\frac{d\mu}{dt} = g_\mu \mu - mY_\mu(\mu) - k_\mu \mu \quad (1)$$

$$\frac{d\mathrm{m}}{dt} = g_{\mathrm{m}} - mY_m(\mu) - k_{\mathrm{m}}\mathrm{m} \quad (2)$$

$$\frac{d\mathrm{B}}{dt} = g_{\mathrm{B}}mL(\mu) - k_{\mathrm{B}}\mathrm{B} \quad (3)$$

where the three functions Y_μ, Y_m, and L which represent respectively the active miRNA degradation rate, active mRNA degradation rate, and translation rate (details in SI section 1.1, Fig. S1-S3). The transcriptional activation and inhibition by SNAIL and ZEB are mathematically represented as a shifted Hill function [50] which is defined shown below,

$$H(X, X_0, n_X, \lambda) = \lambda + \frac{1-\lambda}{1+(X/X_0)^{n_X}} \quad (4)$$

The fold change (λ) represents the magnitude of the activation (λ >1) or inhibition (0=<λ <1), and the sensitivity to the changes in X is represented by the Hill coefficient n (Fig. S3). For readability of the figures, we define the parameter Λ=1-λ such that maximal inhibition occurs when Λ=1 (λ=0) and no inhibition occurs when Λ=1 (λ=1). Previous investigation of the core EMT network by Lu and collaborators showed that the μ_{200}/ZEB module was responsible for the EMT tristability – epithelial (E) with high μ_{200}/low ZEB, mesenchymal (M) with low μ_{200}/low ZEB, and E/M with intermediate μ_{200}/intermediate ZEB, whereas the μ_{34}/SNAIL module mainly acted as a noise buffer [7](see Fig. 1B, and section S2.1 for nullcline analysis).

In a separate line of investigation, a proposed generic regulatory circuit of metabolism AMPK/HIF-1/ROS, provided insight into cancer metabolism plasticity and switching between different metabolism phenotypes. Through this reduced circuit, Yu and collaborators show that cancer cells can acquire at least three different metabolic phenotypes – an "O" state (high AMPK/low HIF-1), a 'W' state (low AMPK/high HIF-1), and a hybrid 'W/O' state (intermediate AMPK/HIF-1) [48](see Fig. 1C).

To couple the regulatory circuits of EMT and metabolism, we did extensive literature search and identified main crosstalks between these two circuits (see Fig. 1A). The crosstalk is obviously bi-directional. For example, regarding EMT regulating metabolism, ROS levels are increased by μ_{34} via downregulating the NRF2-dependent antioxidant capability [51–53], downregulating SOD2 [54], or upregulating the p53 pathway [55,56]. This increase in ROS levels by μ_{34} is potentially more pronounced for mitochondrial ROS (mtROS) versus NADPH oxidase mediated ROS (noxROS), and we will explain in more detail later[51,57]. Next, μ_{200} family members can either upregulate or downregulate Hif1 expression [30]. While miR-429 upregulates HIF-1, both miR-200b [31] and miR-200c [58] downregulate HIF-1 expression. We focus on the negative feedback loop which seems to be present in a larger portion of the miR-200 family members [30,59]. Regarding metabolism regulating EMT, HIF-1 inhibits miR-200b through upregulation of the HIF-1 downstream target ASCL2 [31]. Therefore, there is a mutual inhibitory feedback loop between μ_{200} and HIF-1. Additionally, HIF-1 can directly upregulate SNAIL [60], while AMPK represses the production of SNAIL [61] by activating FOXO3. Similarly, AMPK suppresses ZEB2 by activating FOXO1 [62,63]. Additionally, CREB, after being activated by AMPK via phosphorylation, can transcribe μ_{200} resulting in the upregulation of μ_{200} [64–68]. Please refer to supplementary Table S5 for a detailed description of all crosstalks that have been included in our modeling framework.

The new model we propose here is built by including these crosstalk links so as to couple the circuits of EMT and metabolism respectively. We modify the metabolic circuit such that the mathematical model includes the miRNA regulation of HIF-1 by μ_{200} and confirm that the nullclines and expression of AMPK/HIF-1/ROS for the modified metabolic network model is consistent with results from the model detailed in Ref. [48] (Fig. S4). The full equations for the

dynamics of all components of the circuit are given in SI Section 1.3 and the parameters along with a brief explanation are given in SI Section 1.4.

We started with parameters such that both the EMT and metabolic networks are tristable. This means when the crosstalk are inactive, there are at maximum nine possible combinations of the EMT and metabolic phenotypes: E-W, E-O, E-W/O, M-W, M-O, M-W/O, E/M-W, E/M-O, and E/M-W/O (Fig. 1D, details of numerical integration using the Euler method are given in section S2.2). By including active crosstalks, we can identify crosstalk affects the coupling between EMT states and metabolism states.

While the W state is characterized by high HIF-1/low AMPK and the E state is characterized by high μ_{200}/low ZEB expression, including the crosstalk will quantitatively alter the expression profiles for the various steady states. This means that the use of fixed thresholds to determine the state of the cell is no longer appropriate. Therefore, we use a distance metric normalized by the expression of the decoupled network to classify the generated expression profiles as indicative of one of the nine coupled states (see Section S2.3 for details). With our baseline decoupled network parameters, we show that 1000 initial conditions are large enough to generate consistent percentages of different states (Fig. S5-S7) - with the hybrid states being most populous (W/O and E/M) followed by the W and M phenotypes, followed by the O and E states. This result is just for one set of parameters and others will lead to a different fraction of initial conditions leading to these disparate states.

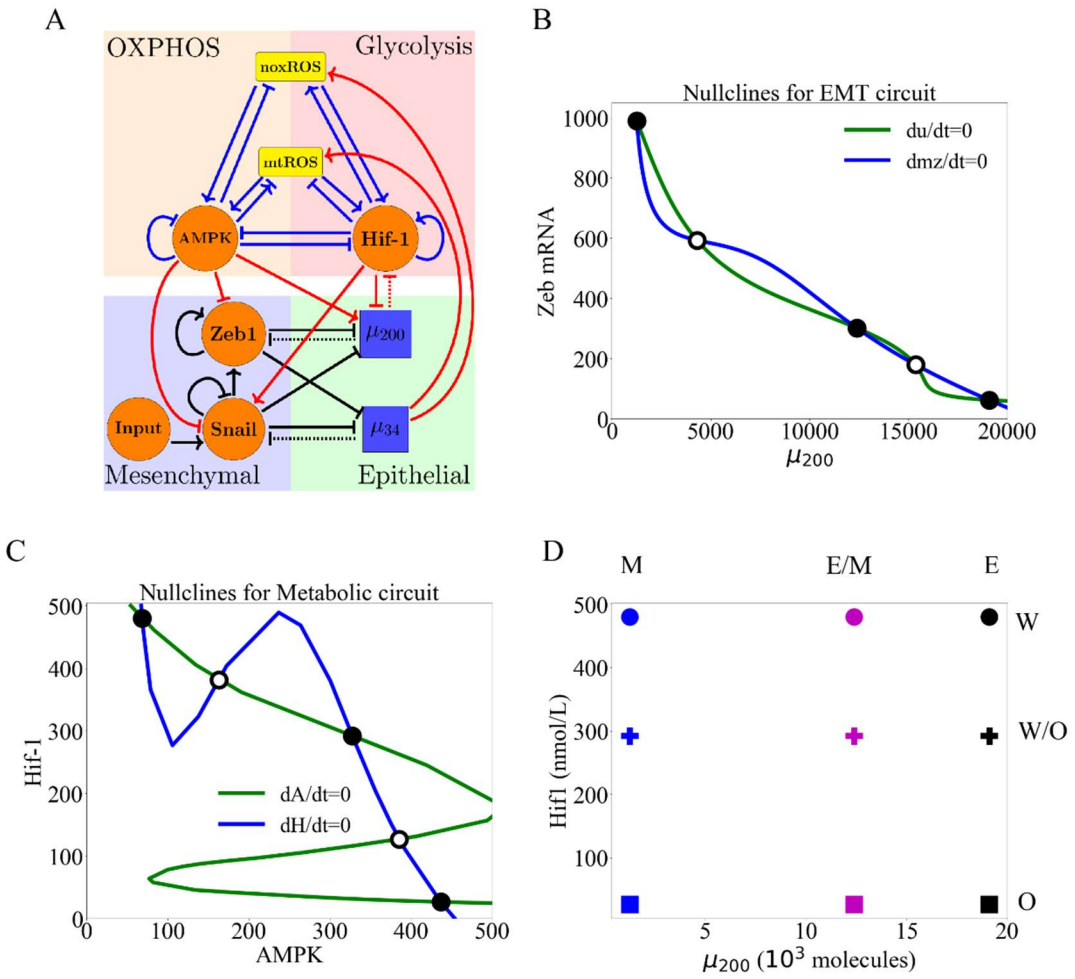

Figure 1. **The coupled EMT/MR circuit results in 9 possible steady states.** With inactive crosstalks all combinations of the steady states of the core EMT and metabolic networks are accessible. **(A)** The network showing the core EMT module (bottom) with regulatory links designated by black, the core metabolic circuit (top) with regulatory links designated by blue, and the crosstalks noted in red. The dashed lines denote miRNA-based regulation. The solid lines denote transcriptional regulation. Regulatory links ending in bars represent inhibition while the arrows represent activation. **(B)** The nullclines of the EMT network. The system is tristable and the three stables states (high μ_{200}/low Zeb, low μ_{200}/high ZEB, and intermediate μ_{200}/ZEB) represent the three states (E, M, E/M) respectively. **(C)** The nullclines of the metabolic network. The system is tristable with three stable states (high AMPK/low HIF-1, low AMPK/high HIF-1, and intermediate AMPK/HIF-1) represent the three to metabolic states (O, W, W/O) respectively. **(D)** The 9 possible phenotypic states when all crosstalks are inactive. The blue, purple, and black markers represent the M, E/M, and E states, respectively. The circle, cross, and square represent the W, W/O, and O states, respectively. Therefore, the coupled E/M-W/O state is represented as a purple cross.

Results

Individual crosstalk can push the downstream circuit towards a single state: Let us start by making just one cross-link active, caused by e.g. an EMT-related microRNA. Now, in our model there is a clearly an unaffected upstream subnetwork (EMT, from where the link originates) and a regulated downstream one. (Note that the model ignores any possible dilution of the microRNA due to its action on ROS; see below).

When noxROS is upregulated by μ_{34} (Fig. 2A), as there is no feedback to the EMT network, the percentages of initial conditions leading to the E, E/M, and M states are unchanged; increasing noxROS enhances the W/O state and consequently the coupled E/M-W/O states are upregulated. In other words, the E/M state becomes more likely to be associated with the W/O state (Fig. 2D). As the level of noxROS increases, the possible coupled states reduce from nine to six, losing first the E-W state, then the E/M-W, and finally the M-W state (Fig. 2B, section S2.4). Further we show that increasing noxROS pushing the W-associated states towards the W/O-associated states, with little change occurring for the O-associated states (Fig. 2C).

Analyzing the states coupled with the W state we found that the M-W state exists for a larger parameter space, compared to the other W-associated states, as the coupling is increased (Fig. 2E). This is as expected since the W state has the lowest μ_{34} level of the metabolism states (Fig. 2E). Similar changes have been observed via the upregulation of mtROS (Fig. S8); the E-W and E/M-W states are also the first suppressed states. Consistent with the effect of upregulating noxROS, upregulating mtROS is also correlated with an increase of the E/M-W/O state. Further, activation of mtROS results in a downregulation of the O state alongside downregulation of the W state, thus stabilizing the W/O state. Together, these results suggest both mtROS and noxROS

may be critical factors in regulating the coupling of two hybrid states – E/M-W/O, and mtROS exhibited a greater increase in the E/M-W/O state than noxROS.

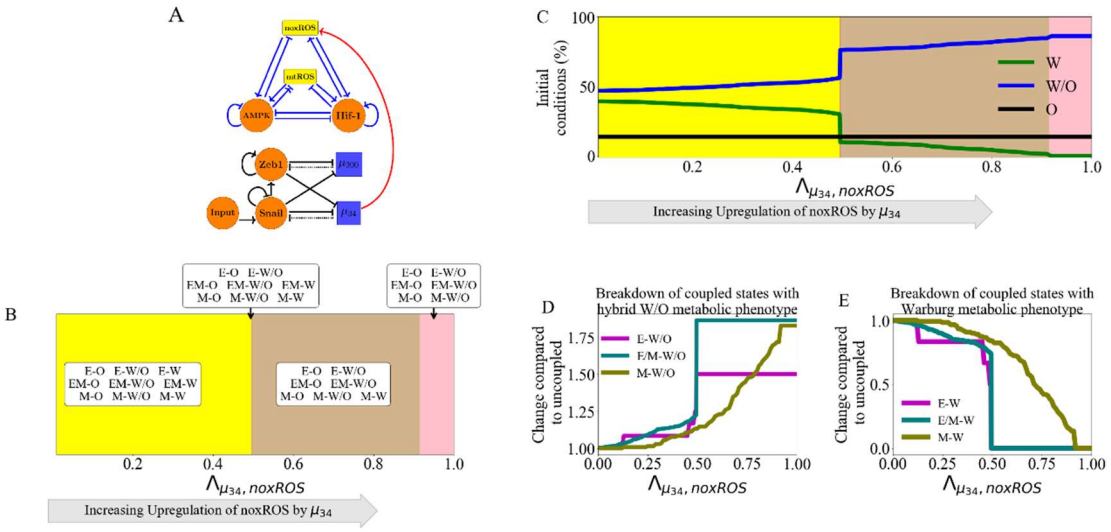

Figure 2. noxROS upregulated by μ_{34} stabilizes the W/O state and enhances the E/M-W/O coupled state. As noxROS is upregulated by μ_{34}, the number of initial conditions leading to the O state is minimally changed, the W state is reduced, and the W/O state is increased. The EMT network is unchanged, as there is no feedback, but the coupling of metabolic states with the EMT states changes, and the E/M-W/O state is upregulated. **(A)** A diagram of the core EMT circuit (left) and the core metabolic circuit (right) connected by the crosstalk μ_{34} upregulating noxROS (red link representing transcriptional regulation). **(B)** Of the nine possible coupled states, as noxROS is upregulated by μ_{34}, there are 4 distinct groupings. All possible couplings of the EMT states (E, M, and E/M) with both the O and W/O states persist for all levels of noxROS upregulation. The coupled states associated with the W state, (E-W, E/M-W, and M-W), are lost as the level of noxROS increases, as shown in the red, tan, and pink regions, respectively. **(C)** The W/O state (blue) is upregulated, W (green) state is downregulated, and O (black) is unchanged. The lines represent the total number of initial conditions leading to the W, O, or W/O states as a function of increasing regulation of noxROS by μ_{34}. (The background colors correspond to the colors representing the possible steady states of (B).) **(D)** Showing the breakdown of the coupled states associated with the W/O state (i.e., E-W/O, M-W/O, and E/M-W/O) compared to the inactive system ($\lambda_{\mu_{34},noxROS} = 1$). The E/M-W/O coupled state is greatly upregulated once $\lambda_{\mu_{34},noxROS} = 0.5$, the M-W/O coupled state is slowly upregulated, and E-W/O is also upregulated. **(E)** Same as (D) but for the coupled states associated with the W state. Once $\lambda_{\mu_{34},noxROS} = 0.5$, both the E-W and M-W states are fully suppressed. The E/M-W coupled state continues to be downregulated until it is fully suppressed near $\lambda_{\mu_{34},noxROS} = 0.1$.

Regulation of HIF-1 affects both subcircuits: While the previous μ_{34} link only affected the downstream network, the miRNA regulation of HIF-1 by μ_{200} can affect both networks. This arises because of the reduction in the microRNA level caused by this coupling. In our model, μ_{200} mediates both the transcription and translation of HIF-1 mRNA, and as a result, μ_{200} can be recycled or degraded. Therefore, while the downstream metabolic network is modulated, the upstream EMT network is also affected via change of μ_{200}. We have defined a function $P_H(\mu)$ to stimulate the above-mentioned effect of μ_{200} on HIF-1 (details of silencing function $P_H(\mu)$ in section S2.5). Note that as we include increased silencing, the first thing which occurs is the restriction of the EMT state; close to $P_H(\mu) = 1$, the only EMT state allowed is M. When we enter this region, all the metabolic phenotypes are allowed. As the μ_{200} mediated regulation of HIF-1 increases, the W/O and W states are suppressed sequentially and the O state is promoted. As the HIF-1 is suppressed by μ_{200}, the degradation of μ_{200} due to binding binding to HIF-1 RNA is reduced and as a results and the W state gradually disappears. When HIF-1 mRNA is fully silenced, only the E-O and E/M-O coupled states remain (Fig. S?). Since the E/M state does not reappear until after the metabolic system has fully transitioned to O, the coupled E/M-W/O state is not observed for all values of μ_{200} silencing HIF-1 mRNA. These results suggest μ_{200} overexpression could promote the O-associated states (O-E and O-E/M) and destabilized the coupled E/M-W/O.

Inclusion of multiple miRNAs of the EMT network can stabilize the W/O metabolic phenotype: We next wish to determine how including links emanating from both μ_{200} and μ_{34} can synergistically drive metabolic reprogramming, and specifically enhance the chances of being in the coupled E/M-W/O state. As mentioned previously, upregulated ROS leads to an increased W/O state (Fig. S8). If both noxROS and mtROS are upregulated by μ_{34} the E/M-W/O

state is further upregulated (Fig. S15). While upregulation of ROS causes an increase in the E/M-W/O state, we showed above that μ_{200} silencing HIF-1 mRNA suppresses the E/M-W/O state; therefore, we may expect some suppression of the E/M-W/O state when including both μ_{200} and μ_{34}. Interestingly, the hybrid E/M-W/O state can be fully suppressed when μ_{200} downregulates HIF-1 and μ_{34}upregulates noxROS, but only partially suppressed when μ_{200} downregulates HIF-1 and μ_{34} upregulates mtROS (Fig. S16). These results suggest the type of ROS present can have different affects on the E/M-W/O state.

The coupled hybrid E/M-W/O state is stabilized if mtROS is upregulated, but noxROS upregulation has minimal effect on the E/M-W/O state. Strikingly, if all three miRNA crosstalk are active (μ_{200} silencing HIF-1 mRNA and μ_{34} upregulating noxROS and mtROS, Fig. 3A) the E/M-W/O coupled state can be suppressed even if the W/O state is present (Fig. 3B). Further, the E/M-W/O state is present for all values of noxROS upregulation but is only present at high values of mtROS upregulation (Fig. 3B). Analyzing the coupled state phases shows the E/M-W/O state is suppressed when mtROS is only slightly upregulated (Fig. 3C). Further, the E and E/M states are associated with the O state when mtROS levels are slightly upregulated. Interestingly, the M state is coupled with O and W/O states while the E and E/M states are only coupled to the W/O state when mtROS is fully upregulated (Fig. 3C). Additionally, depending on the initial conditions, if noxROS is maximally upregulated ($\lambda_{u34,noxROS}$=0), mtROS is upregulated, and HIF-1 is partially silenced by μ_{200} the system can access the hybrid E/M-W/O state (Fig 3D). Also, while mtROS must be upregulated for the system to access the coupled E/M-W/O state, the E/M-W/O state is accessible for all levels of noxROS upregulation (SI Fig S17). There also seems to be a synergistic effect between the three crosstalks resulting in an increased parameter space leading to the E/M-W/O state than what is expected from the

individual crosstalks. Further, the difference in the effect of noxROS and mtROS seems to result from the frustrated regulation of mtROS by HIF-1 and μ_{34}. Therefore, feedback loops between mtROS, HIF-1, μ_{34}, and μ_{200} together control the appearance of the E/M-W/O state.

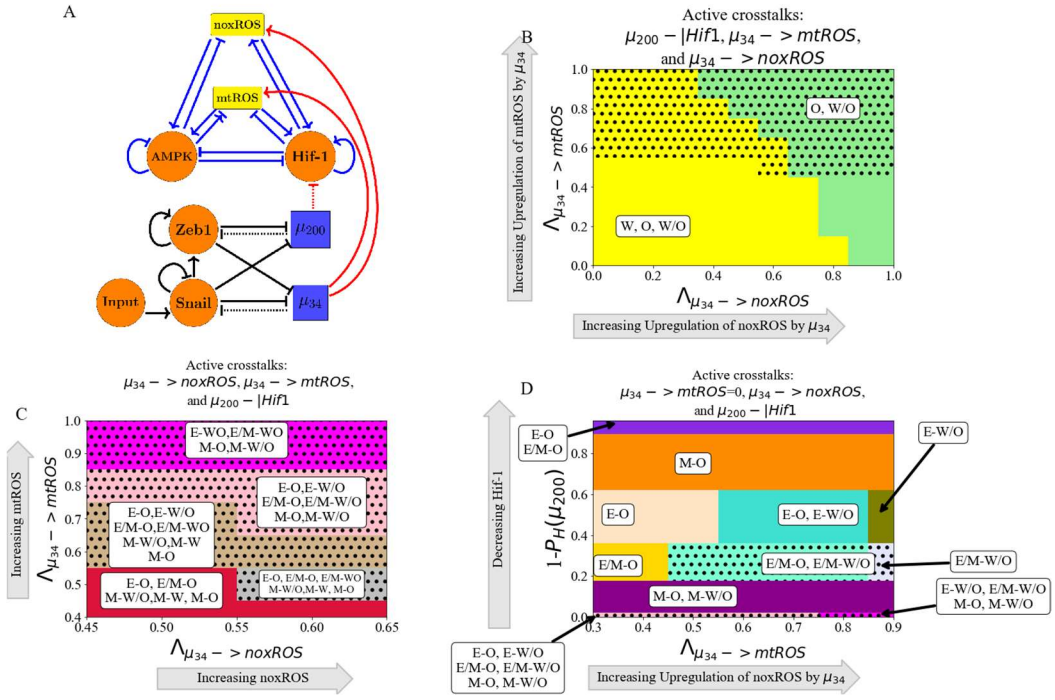

Figure 3. μ_{200} and μ_{34} can upregulate the W/O phenotype. When all three crosstalks from the EMT network (μ_{200}-|HIF-1, μ_{34}-> mtROS, and μ_{34}->noxROS) are active the E/M-W/O state can be upregulated. The E/M-W/O state is accessible when mtROS is high and at intermediate silencing of HIF-1. The level of noxROS seems to have minimal effect. This suggests the μ_{34}/μ_{200}/HIF-1/mtROS axis plays a significant role in stabilizing the hybrid E/M-W/O state. **(A)** Schematic illustration of the coupled metabolic (top) and EMT (bottom) regulatory network with all EMT driven regulatory links active (μ_{34} upregulating mtROS, μ_{34} upregulating noxROS, and μ_{200} silencing HIF-1). **(B)** The phase plane corresponding to all EMT driven regulatory links (network pictured in A). The regulation of HIF-1 by μ_{200} in this phase plane corresponds to the rightmost, blue region of Fig. S? where all metabolic phenotypes are possible. As noxROS is upregulated (right to left), the W state is suppressed. However, as the level of mtROS increases (top to bottom), the black dotted region appears showing the existence of the E/M-W/O coupled state, suggesting mtROS may have a stronger effect on the E/M-W/O state than noxROS. **(C)** The coupled states of (B) when only EMT driven crosstalks are active (μ_{200} downregulating HIF-1 and μ_{34} upregulating mtROS and noxROS). The E/M-W/O state exists when mtROS is upregulated. This is zoomed in on the middle region of (C). **(D)** At maximum upregulation of noxROS ($\lambda_{\mu_{34}->noxROS}$=0), as mtROS increases (x-axis) and HIF-1 is moderately silenced (y-axis) there are regions where the E/M-W/O state is possible (black dotted regions).

Metabolic reprogramming can drive EMT: We next turn to a consideration of information flowing in the other direction, from metabolism to EMT. To elucidate the way in which metabolic reprogramming can drive EMT, we determined the effect of each metabolism-driven crosstalk on the coupled states. First, we analyzed the links in which HIF-1 upregulates SNAIL (Fig. 4A and S9) or inhibits μ_{200} (Fig. S10). As expected, both HIF-1 mediated links push the system towards the M state. Further, both the E and hybrid E/M states are most associated with the O state (when the HIF-1 level is relatively low) while the M state is initially associated with the W state. The correlation between the E-O and M-W states is assumed in much of the literature [29]. Similarly, modulating the EMT-inducing signals such as TGF-β that can activate SNAIL can alter the stability of the E/M state and therefore the coupled states(see Fig. S11). Opposite to the HIF-1 results, AMPK upregulating μ_{200} pushes the EMT network to adopt an E state and suppresses the E/M state followed by the suppression of the M state (Fig. 4B and S12). Similarly, AMPK mediated downregulation of ZEB and/or SNAIL has an analogous effect to AMPK upregulating μ_{200} on the expression of the E/M state and the system saturates near fully epithelial (Fig. S13 and S14). Additionally, when AMPK regulates the EMT circuit alone, the E and M states are still most associated with the O and W states, respectively. However, the E/M state for AMPK driven crosstalk is associated with the W state. This is in direct contract to HIF-1 driven crosstalk in which the E/M state is coupled with O state. The results suggest that neither OXPHOS nor Warburg metabolism is automatically associated with the E/M state and that this state has metabolic plasticity to mix and match different metabolic phenotypes.

The crosstalk between the EMT network and metabolism network play various roles in mediating the coupled states. The μ_{34} mediated upregulation of mtROS or noxROS exhibit consistent upregulation of the E/M-W/O state and suppression of the E-W and E/M-W coupled

states. The phases of the coupled states are also very similar when HIF-1 inhibits μ_{200} or upregulates Snail, first suppressing the E-W, E-W/O, and E/M-W states and stabilizing near fully mesenchymal. However, the E/M-W/O state does exist for a larger portion of the parameter space when HIF-1 inhibits μ_{200} (Fig. S9 and S10). Lastly, the AMPK driven crosstalks (inhibiting ZEB or SNAIL or upregulating μ_{200}) are initially very similar, suppressing first the E/M-O and E/M-W/O states. In fact, the phases are nearly identical when AMPK inhibits ZEB or SNAIL (Fig. S13 and S14). However, AMPK upregulating μ_{200} has slightly different effect on the coupled states before saturating at epithelial (Fig. S12). These similarities between the effect of different crosstalk suggests a degree of consistency in how EMT drives metabolic reprogramming, and vice versa.

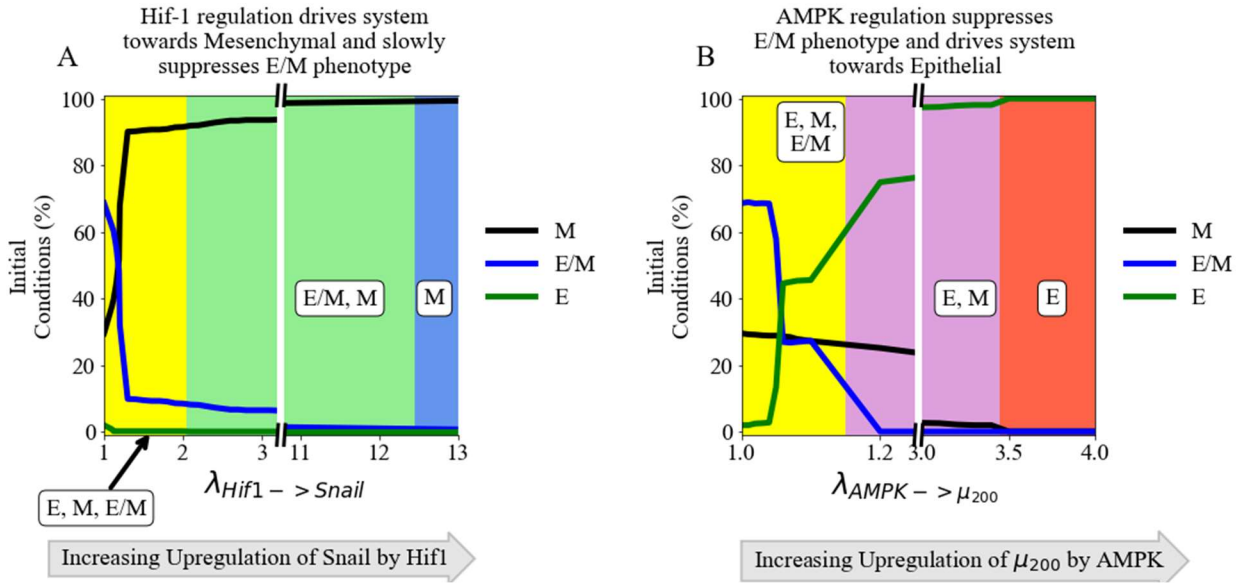

Figure 4. The role of metabolism in driving EMT. HIF-1 mediated crosstalks drive the EMT circuit towards the M state, while AMPK mediated crosstalks drive the EMT network towards the E state. Neither type of crosstalk alone can stabilize the E/M state, but the E/M state persists longer for HIF-1 controlled crosstalks. **(A)** The number of initial conditions leading to an E/M, M, or E state as HIF-1 upregulates SNAIL. The hybrid E/M state is suppressed quickly as the system is driven towards the M state. **(B)** The number of initial conditions leading to an E/M, M,

or E state as AMPK upregulates μ_{200} and drives the system towards epithelial. The E/M state exists for larger portions of the parameter spaces for HIF-1 regulation than for AMPK-mediated crosstalks.

TFs of the metabolic network can stabilize the E/M metabolic phenotype: There are two distinct events at play when the metabolic network regulates the EMT circuit. AMPK regulation quickly suppresses the E/M state and pushes the system towards the E state whereas HIF-1 regulation can allow the system to maintain the E/M state for a range of strengths while ultimately pushing the system towards the M state (Fig. 4A and 4B). As AMPK and HIF-1 push the system towards opposite states, having active links emanating from both should push the circuit towards a hybrid state. That is exactly what happens when at least one of the three AMPK crosstalks and at least one of the two HIF-1 crosstalks, although the exact values of where the E/M-W/O state exists depends in detail on the type of regulation (Fig. S18). Additionally, if AMPK and HIF-1 target different EMT TFs, the E/M-W/O state may exist in larger parameter spaces than if they target the same EMT TF (Fig. S18), suggesting multiple crosstalks should be active and multiple gene regulators should be targeted to stabilize the E/M-W/O state. If all crosstalks involving AMPK and HIF-1 regulating the EMT circuit are active (Fig. 5A) then there are significant regions in which the E/M state exists (Fig. 5B). However, when analyzing the system for the existence of the E/M-W/O state, it only exists in a small region where μ_{200} is minimally upregulated. Moreover, HIF-1 driven crosstalks are able to maintain the E/M state longer than AMPK driven crosstalks suggesting, the reduced regions of E/M-W/O existence is likely due to the suppression of the E/M state by AMPK regulated crosstalks, as mentioned above (see Fig. S12-S14). This suggests HIF-1 driven crosstalk is more strongly correlated with

the E/M state than AMPK driven crosstalk, in agreement with a recent study based on publicly available expression data [69].

To stabilize the E/M state, both AMPK and HIF-1 crosstalk are necessary, and if all EMT regulating crosstalks are active then there are regions where the E/M-W/O state exists. Additionally, the E state is typically coupled to the O state (E-O), the M state is associated with the W state (M-W), and when the E/M state is present it is typically associated with the hybrid W/O state (Fig. 5C). In fact, for any system, if there are only three coupled states available and each has a distinct phenotype of the EMT and metabolic networks, then the only possible set of states is E-O, M-W, and E/M-W/O. This behavior represents the full coordination of EMT and metabolism and suggests clusters of migrating cells utilize a combination of aerobic glycolysis and OXPHOS. Given tumors are metabolically heterogeneous, this result suggests the topology and parameters of the system may only represent certain microenvironments and is a limitation of our study.

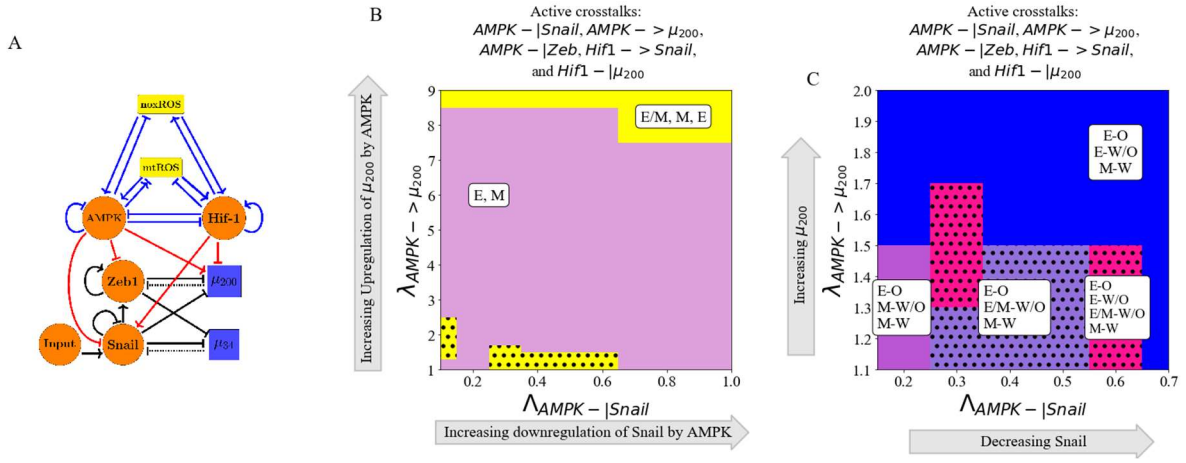

Figure 5. AMPK and HIF-1 cooperate to upregulate the hybrid E/M state. When all HIF-1 and AMPK controlled crosstalks are active (HIF1->Snail, HIF1-|μ_{200}, AMPK-|Snail, AMPK-|Zeb, AMPK-> μ_{200}) the E/M-W/O state can be stabilized. HIF-1 driving the network to mesenchymal and AMPK driving the system towards the E state results in HIF-1 and AMPK cooperatively stabilizing the E/M state. Once stabilized, the E/M state is coupled with the W/O state (i.e., stabilizing the coupled E/M-W/O state). **(A)** Schematical illustration of the network

showing how metabolism drives EMT. ZEB is inhibited by AMPK, SNAIL is upregulated by HIF-1 while being downregulated by AMPK, and μ_{200} is upregulated by AMPK while being inhibited by HIF-1. **(B)** The phases plane of potential EMT states when all metabolic driven crosstalks are active. The E/M state is only accessible when $\lambda_{AMPK-|\ \mu200}$ is near 1 or very high (i.e., at the extremes of regulation). **(C)** The coupled states when the EMT circuit is regulated by the metabolic circuit (AMPK-|SNAIL, AMPK-|ZEB, AMPK->μ_{200}, HIF-1 -|μ_{200}, HIF-1 -> SNAIL). The results suggest a direct correlation between the E, E/M, and M states to the O, W/O, and W states, respectively.

The Hybrid E/M-W/O phenotype: Recently, it has been suggested that the most metastatic cancer phenotype is characterized by the hybrid E/M state and hybrid W/O state[29]. Therefore, it is now useful to focus our discussion onto how the crosstalk between EMT and metabolism regulatory networks specifically affects the E/M-W/O state and the possibility that it could be the only possible coupled state for certain parameter spaces. From our analysis of activating individual crosstalks, we deduce that two competing metabolic driven crosstalk and one competing EMT driven crosstalks would be minimally necessary to fully stabilize the E/M-W/O state and suppress all other coupled states.

In detail, the hybrid E/M-W/O state can be stabilized when AMPK downregulates SNAIL, HIF-1 downregulates μ_{200}, and μ_{34} upregulates mtROS. The E/M-W/O state exists in much of the space and is increased in prevalence when SNAIL is significantly repressed by AMPK ($\lambda_{AMPK-|\ SNAIL}$=0.2), mtROS is upregulated, and μ_{200} levels have been moderately downregulated (Fig 7A and S19A). Further, instead of HIF-1 downregulating μ_{200}, increasing SNAIL levels can promote the E/M-W/O state to become even more prevalent (Fig. 6B and S19B). While, the E/M-W/O state was stabilized in both cases (Fig. 6A and B), neither was able to fully stabilize the E/M-W/O state and suppress all other states.

It is possible to suppress all states except the coupled E/M-W/O state with just three regulatory links; HIF-1 inhibiting μ_{200}, μ_{34} upregulating mtROS, and modulating the EMT-inducing signal (Fig. 6C and S19C). In fact, no other combination consisting of only three regulatory links seems to enable only the E/M-W/O state(Fig. S?). Additionally, this region which only includes the E/M-W/O state persists even if all remaining crosstalks are activated (Fig. 6D and S19D).

Looking at the proximal phases next to the one with just E/M-W/O suggests that stabilization of the E/M-W/O state requires mutual activation between metabolic reprogramming and EMT. When the E/M-W/O state can be the only available state (Fig. 6C and 6D), the surrounding phases are the same whether only three crosstalks or all crosstalks are active (E-O and E-W/O), suggesting there may be a sequential path to generate the E/M-W/O state. Further, if the E/M-W/O state is not the only allowed state (Fig. 6A and 6B), the surrounding phases include M-coupled states (M-O, M-W/O, and M-W) as well as E-coupled (E-O and E-W/O). Together the results suggest that to reach the E/M-W/O state for epithelial cancer, first metabolic reprogramming should occur and the E-W/O state should be acquired, followed by a partial EMT (E/M-W/O). Additionally, the persistence of the E/M-W/O state suggests there might be other combinations of crosstalks that generate phases where only the E/M-W/O state is possible, although it is outside the scope of this manuscript to find all possible combinations of crosstalks that can enable only the hybrid E/M-W/O coupled state. However, based on these results, we would expect HIF-1 suppressing μ_{200} and μ_{34} upregulating mtROS to be prominent among all such combinations.

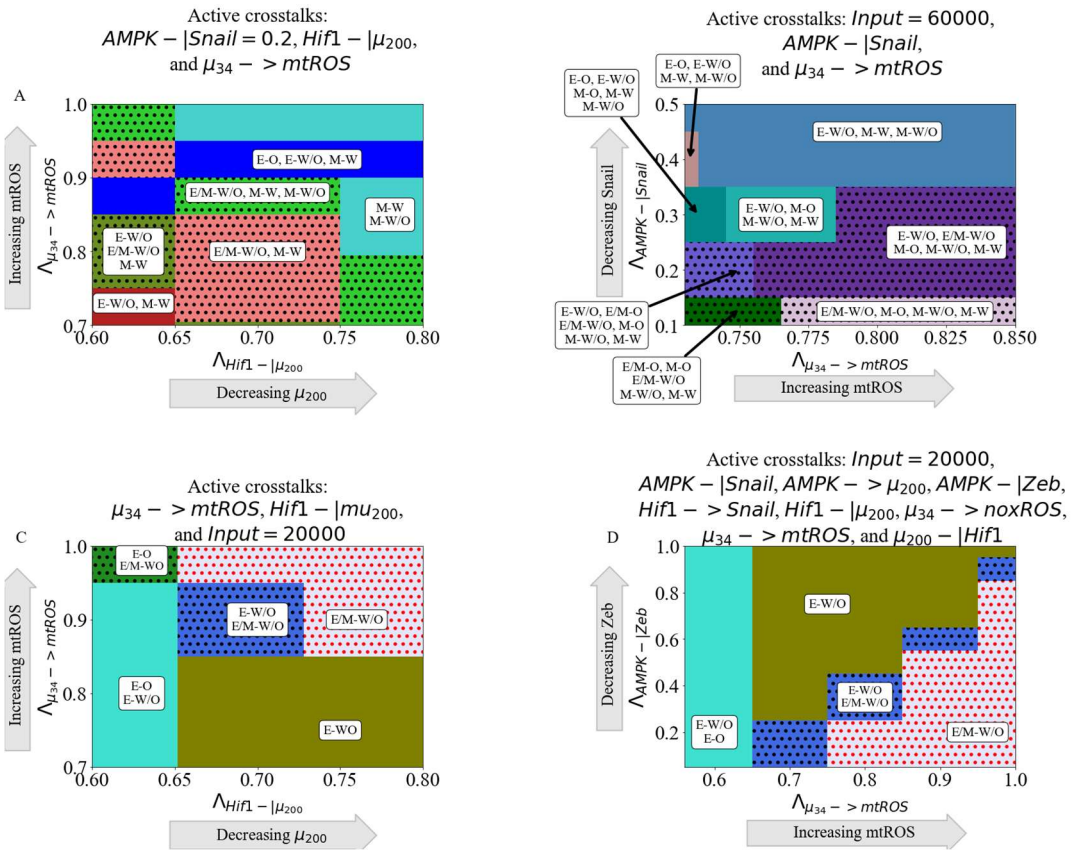

Figure 6. The coupling of the EMT and metabolic regulatory networks can enable a coupled hybrid E/M-W/O state. Minimally, three links (one effecting the metabolic network and two controlling the EMT network) are necessary to suppress all coupled states except the E/M-W/O state. Many combinations of crosstalk can upregulate the E/M-W/O state, but to enable the E/M-W/O state to be the only stable state, three crosstalk are necessary – μ_{34} upregulating mtROS, HIF-1 inhibiting μ_{200}, and EMT-inducing signaling that regulate SNAIL. **(A)** Phase diagrams of the coupled states when considering three crosstalk; the Input=60000 molecules, AMPK downregulates SNAIL, and μ_{34} upregulates mtROS. The E/M-W/O state is upregulated when mtROS levels are increased. **(B)** The phase diagram of the coupled states when considering the inhibition of SNAIL by AMPK ($\lambda_{AMPK\text{-}|\ SNAIL}$=0.2), HIF-1 inhibiting μ_{200}, and μ_{34} upregulating mtROS. The E/M-W/O state is upregulated for some regions. **(C)** When considering the bi-directional regulation between EMT and metabolism by the three minimally necessary regulatory links, there are parameter regions in which the only possible coupled state is the E/M-W/O state. **(D)** When all crosstalks are active there are regions where only the E/M-W/O state exists. Similar sets of coupled states in (C) and (D) suggest a preferential pathway to drive the system towards the hybrid E/M-W/O coupled state.

Hybrid phenotypes are enabled by crosstalk in cells initially without the E/M or W/O state:

We have showed that the E/M and W/O states are often connected, the population in the E/M-

W/O state can be expanded depending on the relative strength of various links, and there are parameter sets with only the hybrid E/M-W/O state available and all other coupled states suppressed. Next, to investigate whether the crosstalk between EMT and metabolism enables cancer plasticity e.g., by acquiring the hybrid states. We simulate scenarios where the individual EMT and metabolism networks cannot acquire a hybrid state, corresponding to normal physiological conditions where we expect most cells will be restricted to a binary choice of E versus M and W versus O [70]. Then we systematically analyze whether any crosstalk can enable the hybrid state to emerge.

First, we confirmed both the EMT network and metabolic network are independently bistable when the crossstalk is inactive(Fig. S20), and ensured the solutions from the initial conditions were evenly divided between the steady states (Fig. S21-S22). We can then proceed to determine the consequences if EMT and metabolism mutually regulate each other.

As already mentioned, the EMT network can drive metabolic reprogramming via microRNA-mediated links. We first kept the metabolic circuit as a bistable system where only W and O are the available stable states, i.e., no hybrid W/O state when the cross-talk is inactive. Then we analyzed the coupled states considering links - μ_{34} upregulating mtROS, μ_{200} downregulating HIF-1, or μ_{34} upregulating noxROS. We found that the metabolic circuit becomes tristable, i.e., the hybrid W/O state emerges, when mtROS is upregulated by μ_{34} (Fig. 7A) but doesn't appear if only noxROS is upregulated or μ_{200} is downregulated (Fig. S23). Additionally, the upregulation of mtROS by μ_{34} can further stabilize the coupled E/M-W/O state so that all E/M states become coupled with the W/O states. Furthermore, the upregulation of noxROS in the bistable circuit causes an increase in the frequency of the O state, in contrast to an increase of the frequency of the hybrid W/O state in the tristable circuit (Fig. S23 compared to

Fig. 2). This suggests, noxROS may play a context-dependent role on the coupled state, while mtROS often stabilizes the E/M-W/O state.

Next to see whether metabolic reprogramming can enable the emergence of the hybrid E/M state, we kept the metabolic circuit as a tristable circuit and set the EMT network to be bistable (i.e., unable to acquire a hybrid E/M state alone). Then we investigated the effects of the following cross-talk, HIF-1 inhibiting μ_{200}, and HIF-1 upregulating SNAIL. When analyzing the inhibition of μ_{200} by HIF-1, we found that the coupled EMT-metabolism network is able to quickly generate the E/M-W/O state before it is once again suppressed (Fig. 7B). However, the E/M state persists but is coupled to the O state (E/M-O). Additionally, when analyzing the effect of HIF-1 upregulating SNAIL, we found that the E/M-W/O state is only generated when SNAIL is moderately upregualted (Fig. S24). Furthermore, both HIF-1 inhibiting μ_{200} and HIF-1 upregulating SNAIL can stabilize the system in the phase - (E/M-O, M-W, M-O, M-W/O), where the hybrid E/M state can be stably maintained. This suggests the master regulator of glycolysis, HIF-1, can drive cells towards the hybrid E/M state. Conversely, an individual AMPK-mediated crosstalk is unable to generate the hybrid E/M state and saturates in the epithelial phase (Fig. S24), as seen in the tristable circuit. Additionally, as with the tristable networks, the coupled hybrid E/M-W/O state can be stabilized by two competing crosstalk, such as AMPK upregulating SNAIL and HIF-1 downregulating μ_{200} (Fig. S25). These results suggest HIF-1 can strongly affect and drive EMT into a hybrid E/M state while AMPK can only help stabilize the E/M-W/O state if it is already present.

When both the EMT and metabolism networks are in the parameter regime where hybrid E/M or hybrid metabolism state is not available, the cross-talk can enable the emergence of these hybrid states. Recall that for the coupled tristable circuits, the simplest set of crosstalk with a

parameter region that suppressed all coupled states except the E/M-W/O state consisted of three regulatory links: (1) HIF-1 inhibiting μ_{200}, (2) μ_{34} upregulating mtROS, and (3) EMT-inducing signaling acting on SNAIL. When these same links are active for the bistable EMT and metabolism circuits, the results are qualitatively very similar to the tristable circuit results (Fig. 7C and S26 compared to Fig. 6C). The E/M state is only possible near full inhibition of μ_{200} and the W/O state is possible when mtROS is greatly upregulated. Further, the system must be near maximum regulation (i.e., $\lambda_{HIF\ ,\mu_{200}}$ and $\lambda_{\mu_{34},mtROS}$ must be close to zero) to generate the region where only the coupled hybrid E/M-W/O state is available. Additionally, the nearby phases surrounding the phase containing only the E/M-W/O state (E-O and E-W/O) is similar relative to those of the tristable circuit, further supporting a progression that must be followed to reach the E/M-W/O state.

Overall, we showed that if the metabolic network is bistable (W or O states) and the EMT network is tristable (E, E/M, or M states), μ_{34} upregulating mtROS can generate the W/O state and upregulate the E/M-W/O state. Conversely, if the EMT network is bistable (E or M) and the metabolic network is tristable (W, O, or W/O), a HIF-1 controlled crosstalk can briefly generate the E/M state and stabilize the E/M-W/O state. If both networks are bistable, the same three links as the tristable case (μ_{34}-> mtROS, HIF1-|μ_{200} and reducing the EMT-inducing signal) generates the E/M-W/O state and suppresses all other coupled states.

We also identified a sequential event to reach the coupled hybrid E/M-W/O state. starting from an E state, which typically associated with an O state, then transitioning from E-O to E-W/O, and finally transitioning to the coupled hybrid E/M-W/O state. In other words, cells may first reprogram their metabolism from O to the hybrid W/O state, followed by the initiation of EMT and a transition to the hybrid E/M state, thus exhibiting the E/M-W/O state.

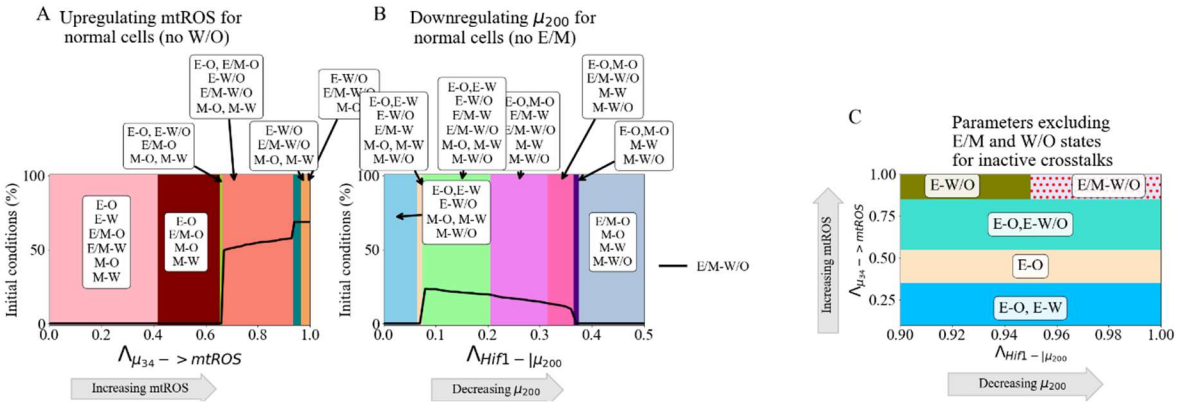

Figure 7. Crosstalk can generate the hybrid states. The activation of a single crosstalk (μ_{34}-> mtROS, HIF1 -> SNAIL, or HIF1 -|μ_{200}) can generate the hybrid state of the downstream network (W/O, E/M, or E/M), respectively. **(A)** The phase diagram showing coupled states where W/O is not available initially when the crosstalk is inactive ($\lambda_{\mu_{34}->mtR} = 1.$). Initially, only the O and W states can be accessed with an increase in the frequency of the O state and decrease of the W state. Once $\lambda_{\mu 34} = 0.35$, there is a sharp change with the hybrid W/O state becoming the most often occupied state. **(B)** The phase diagram of coupled states when the hybrid E/M state is not available initially when the crosstalk is inactive. As the inhibition increases ($\lambda_{Hif1-|\mu_{200}}$ goes towards zero), the system goes from only the E and M states available to regions in which the E/M state is accessible. **(C)** Combining the models from (A) and (B), we generate a model which only has 4 possible coupled states if the crosstalk is inactive (E-O, E-W, M-O, and M-W). At maximum upregulation of mtROS and downregulation of μ_{200}, the E/M-W/O state is the only one accessible, similar to Fig. 6C.

GRHL2 and OVOL can stabilize the coupled E/M-W/O state: Previously, we have reported there are transcription factors, such as OVOL and GRHL2 that can stabilize the hybrid E/M state [14,49], referred to as phenotypic stability factors (PSFs) of the hybrid E/M state. We are curious whether these PSFs of the hybrid E/M state may also have a role in stabilizing the coupling of the hybrid E/M state with the hybrid W/O state. Since GRHL2 upregulates ROS in a manner similar to μ_{34} [71], GRHL2 may also stabilize the W/O state. Therefore, we extended the original coupled EMT-metabolism network to include these PSFs (Fig. 8A, parameters and modified equations of the PSF stabilized network are in Section S1.6). When the crosstalks are

inactive, we find the PSF stabilized network can either be in the E/M-W/O or E/M-O state, and more than 90% of initial conditions lead to the hybrid E/M-W/O state (Fig. S27).

When a single crosstalk is active in the PSF coupled network, the behavior is as expected, with the E/M-W/O state persisting for larger parameter spaces relative to the coupled network without the PSFs. For instance, the hybrid E/M-W/O state exists for the entire parameter space when only one of the following crosstalk is active - AMPK downregulating SNAIL, AMPK upregulating μ_{200}, μ_{34} upregulating mtROS, or μ_{34} upregulating noxROS (see Fig. S28). Additionally, we can assume any EMT-mediated upregulation of mtROS or noxROS will have a similar effect by stabilizing the W/O state (and also the E/M-W/O state). The parameter space enabling the phases where the E/M-W/O state exists is also increased when these PSFs are present when the following crosstalk is active- HIF-1 downregulating μ_{200} or HIF-1 upregulating SNAIL (Fig. S28).

Next, we studied the effect of the PSFs on the E/M-W/O state when multiple crosstalks are active. If two competing crosstalks acting on the EMT circuit are active (e.g., one HIF-1 and one AMPK driven regulation active), then the E/M-W/O state is available for most of the parameter space (Fig. 8B). By comparing how the phases change as the foldchange increases, the regulatory crosstalks controlled by HIF-1 seem to have a stronger affect than the AMPK crosstalks and can push the system towards the M state, as shown by the presence of the M-W/O state as μ_{200} is inhibited by HIF-1. This corresponds with results from the tristable and bistable coupled networks where AMPK upregulating μ_{200} seems to have a weaker effect, specifically on the stability of the E/M-W/O state, than HIF-1 downregulating μ_{200}. Lastly, we activate all three crosstalks that were shown in the tristable and bistable networks to suppress all states except the E/M-W/O state (i.e., μ_{34} upregulating mtROS, HIF-1 downregulating μ_{200}, and including the

EMT-inducing signaling acting on Snail). Once again, there is a phase where only the E/M-W/O state can exist (Fig. 8C). Furthermore, this phase exists in a far larger region in the presence of the PSFs (Fig. 8C and S29) relative to the absence of the PSFs (the light red region at the top right corner of Fig. 8D is the location of the E/M-W/O when no PSFs are present). The large red region on the right side of Fig. 8D is the additional parameter space where the E/M-W/O state is stabilized when the PSFs are coupled with the network. Further, the coupled states in the phases surrounding the region of E/M-W/O are the same as those in the bistable networks (E-W/O and E-O), and also appear in the analysis of the tristable network. These results confirm the PSFs can stabilize not only the E/M state but also stabilize the coupling of the hybrid E/M state with the hybrid W/O state, i.e., the E/M-W/O state.

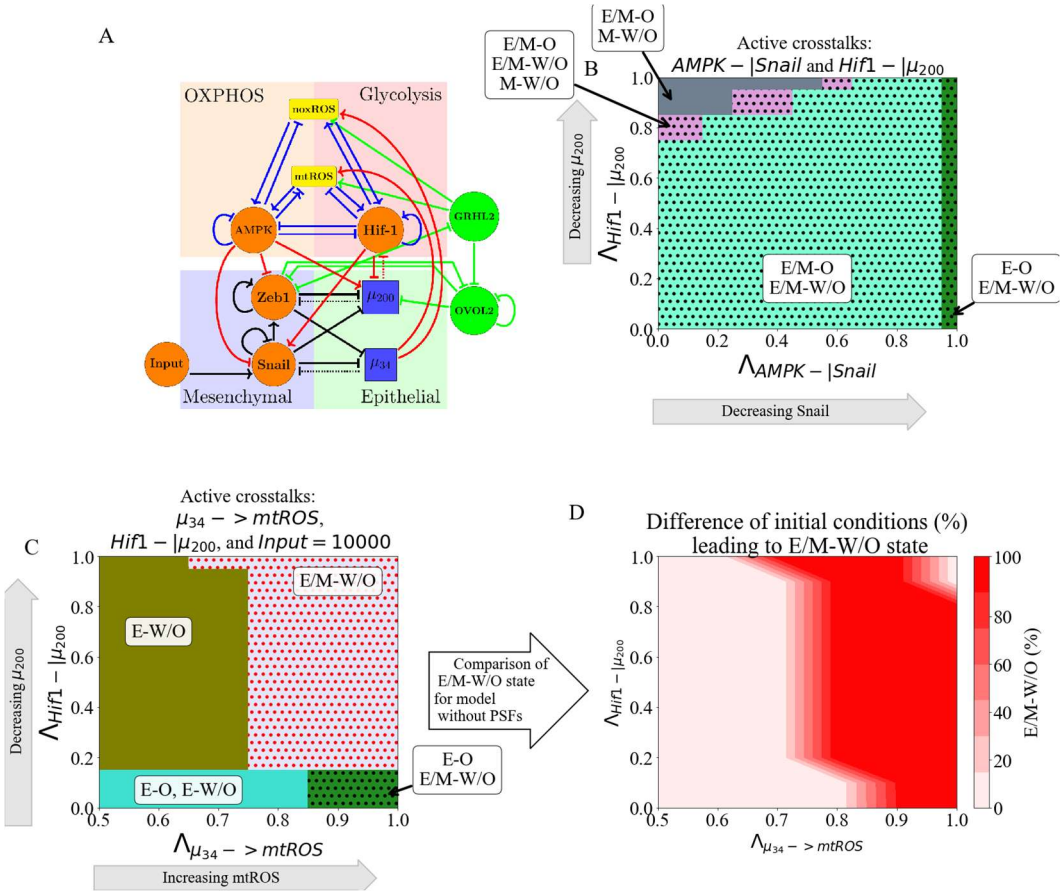

Figure 8. PSFs stabilizing the E/M state can stabilize the association of the E/M state with the W/O state. Including the PSFs GRHL2 and OVOL2 further stabilizes the E/M-W/O state. Once again, the three links (μ_{34}-> mtROS, HIF1-|μ_{200}, and reducing the EMT-inducing signal) suppresses all states except the E/M-W/O state and increases the parameter regime of the phase. **(A)** The coupled EMT-metabolism network including GRHL2 and OVOL2. **(B)** The phase diagram of the coupled states when the PSFs are present. E/M-W/O state is present in a larger parameter space due to the PSFs stabilizing the E/M state even when AMPK downregulates SNAIL and HIF-1downregulates μ_{200}. **(C)** The phase diagram of the coupling states when the crosstalks – EMT-inducing signal acting on SNAIL is set to 10K, μ_{34} upregulating mtROS, and HIF-1 downregulating μ_{200}– are present together. The phase where the E/M-W/O state is the only possible coupled state is significantly enlarged compared to the coupled network without PSFs. **(D)** The difference in the frequency of the E/M-W/O state between (C, PSFs present) and the original model (Fig. S29B, PSFs are not present). The dark red region shows the phases in which only the PSF stabilized model can enable the E/M-W/O state. The light red in the bottom left corner near (0,0.1) is the only region in which the E/M-W/O state is the only stable state irrespective of the presence of PSFs. The light red on the right side is where neither model, PSFs present or not, can generate the E/M-W/O state.

Discussion

This work has presented a comprehensive guide to the effects generated by various regulatory links that couple core circuits responsible for the epithelial-mesenchymal transition and the choice of glucose metabolism. We started by considering the activation of individual links and discovered that these can have rather distinct effects. This made it challenging to study the combined effects of simultaneously including several links. This challenge was again compounded by having to consider the external signals that set the parameters of, and thereby bias, the individual EMT and metabolic subsystems and their interaction. We therefore decided to focus primarily on E/M-W/O states, as we expect that these cells are the most metastatically capable.

Some of our important findings include:

- When the miRNA of the EMT network regulate the metabolic network, the E/M-W/O state can be upregulated with just a single crosstalk. However, when the TFs of the metabolic network regulate the EMT network, a minimum of two crosstalks with opposite effects must be active. Additionally, if crosstalks in both directions are active it is possible to suppress all states except the E/M-W/O state.

- The stabilization of the most plastic E/M-W/O state can be facilitated by the addition of "phenotypic stability factors' (PSFs) to the baseline circuit. Interestingly, one can obtain such states even under conditions when the individual core circuits do not generate hybrid states on their own.

- Lastly, to suppress all coupled states except the hybrid E/M-W/O, our results indicate a progression must be followed; starting from an E-O state, metabolic reprogramming can push the state to E-W/O, followed by partial EMT to stabilize the hybrid E/M-W/O state.

Our results suggest that mtROS is critical to the metabolic activation of EMT. In agreement with our results, recent experimental work has posited that mtROS may drive EMT [72], control cancer invasiveness [73,74], and have a much stronger role than noxROS [51,72]. Also, while it is generally accepted that HIF-1 is important to metabolic reprogramming [22] and triggering EMT [9], the connection between HIF-1, mtROS, and cancer aggressiveness has also been suggested [75]. Indeed, our results suggest the mtROS/HIF-1 axis is critical to stabilizing the highly aggressive E/M-W/O state. Additionally, ROS and HIF-1 expression is controlled by the miRNAs of the EMT network, μ_{34} and μ_{200}, confirming the importance of miRNAs in cancer metastasis [76]. Consequently, our results suggest the existence of a feedback loop between μ_{34}, μ_{200}, HIF-1 and ROS may be critical to stabilizing the E/M-W/O state associated with metastasis and tumorigenesis.

In agreement with other studies [29] our findings indicate that all else being equal, undergoing EMT tends to correlate with using additional glycolysis. This result is consistent with a recent study based on published expression data from public databases [69]. The result is somewhat surprising given the widespread impression that primary tumors often exhibit the Warburg effect, possibly because of their need to limit the amount of ATP produced in favor of maximizing growth (see [77] and references therein). However, this finding is consistent with the general idea that moving from E to E/M is connected with increasing stemness, and stem-like capabilities often rely on glycolysis. Resolution of this issue must await a more precise idea of

the phrase ‘all else being equal”. For example, we have ignored external driving of Hif-1 as would clearly occur in hypoxic environments. Mesenchymal cells that reduce proliferation and have to traverse the ECM should switch to more OXPHOS, whereas ones that become quiescent in a hypoxic metastatic niche should favor glycolysis.

In line with the above, this work is merely a first step, and it is quite likely that incorporating additional pathways may be necessary to improve our understanding of the mutual activation between EMT, metabolic reprogramming and other physiological factors. One such factor is NRF2. Coupling the KEAP1-NRF2 pathway to Notch signaling has been connected to the E/M state [45], and NRF2 is also an antioxidant that must be downregulated to increase ROS concentration [51–53]. Perhaps the metabolic phenotype of NRF2-stabilized E/M cells could correspond to a hybrid W/O state [28]. Additionally, the p53 pathway seems to upregulate noxROS and interfere with EMT [55,56]. Similarly, the E/M-W/O state was stabilized when the EMT-inducing signal was modulated confirming the tumor microenvironment and other signals, such as TGF-β and NF-κβ, may be important to generating the E/M-W/O state [78,79]. While we have tried to ensure our parameters are in a biologically relevant range (utilizing values from literature whenever available), one limitation of this study is knowing whether these results are translatable to experimental cancer studies. Therefore, the significance of the mtROS/HIF-1/μ_{200}/μ_{34}/SNAIL feedback loop could be experimentally tested by reducing the antioxidant factor SOD2, inducing hypoxia, and treating the cells with NF-κβ. Overall, the importance of external signaling in our model is in conceptual agreement with a hypothesis by Sciacovelli and Frezza that, in an adverse tumor microenvironment, metabolic reprogramming drives EMT to allow cells to find more favorable metabolic niches [42].

Understanding how the E/M-W/O state is stabilized by the crosstalk connecting EMT and metabolic reprogramming could be of vital importance to disrupt metastatic processes. Interestingly, the model we have proposed predicts EMT can drive metabolic reprogramming or vice versa, a question that remains unanswered [29,33–39,42–44]. In both instances, the hybrid E/M and hybrid W/O states are coupled. A recent study showed EMT may not always be correlated with the Warburg/OXPHOS metabolic axis, but when the two networks are coupled our model agrees with the identified experimental correlations between high glycolysis metabolism, high or low OXPHOS metabolism, and the E/M state [69]. Our model is consistent with these findings, predicting the hybrid E/M state is coupled to high glycolysis/high OXPHOS (hybrid W/O state). Additionally, HIF-1 (a marker of glycolysis) is strongly associated with EMT while AMPK (a marker of OXPHOS) has a much weaker effect, suggesting the E/M state can be stabilized if HIF-1 (glycolysis) is upregulated, as we proposed above. Notably, in its current form, our model is unable to explain the cases wherein low glycolysis metabolism is correlated with EMT. However, extending the model to explicitly include the coupling with glycolysis, glucose oxidation, and fatty acid oxidation metabolic pathways[80] may be able to explain the low glycolysis states of Ref. [69].

The overall goal of this project is to understand the entirety of cancer metastasis, including cell migration. Previous work has shown that cancer cells can transition from collective migration of E/M cells to migration via amoeboid cells [9,81]. Additionally, the generation of the amoeboid cells is partially due to interaction with the extracellular matrix and regulation by the RHO-ROCK signaling network [81,82]. A recent study showed that AMPK can suppress the metastatic potential of amoeboid cancer cells [82]. Our work shows AMPK may not be critical to stabilizing the E/M-W/O state, suggesting that there is a transition point in the

AMPK/HIF-1 metabolic axis dependent on the dominant signaling network. Inclusion of RHO-ROCK signaling could provide a detailed understanding of cancer cell migration. Further, this would confirm whether the weaker effect of AMPK, compared to HIF-1, in our current model is truly a topological effect, as expected.

The results of our model suggest that metabolic reprogramming can indeed drive EMT, but metabolic reprogramming does not have to be complete before EMT begins; this allows the most aggressive E/M-W/O state to be stabilized. Further, to ensure only the E/M-W/O state is accessible, the system follows a progression from the E-O state, undergoes metabolic reprogramming while maintaining epithelial characteristics (E-W/O coupled state), begins EMT and stabilizes in the E/M-W/O state. Strikingly, the prevalence of the E/M-W/O state is increased by EMT-metabolism crosstalk regardless of phenotypic availability (i.e., whether the initial system is fully E/M-W/O or only E-O, E-W, M-O, and M-W). Therefore, our current model provides an explanation for the mutual activation of metabolic reprogramming and EMT, depending on the initiating signal.

The mutual activation of the epithelial-mesenchymal transition and metabolic reprogramming stabilizes a highly aggressive E/M-W/O state which may be critical to cancer metastasis. Suppressing all coupled states except the E/M-W/O state requires only three links, suggesting the μ_{34}/μ_{200}/HIF-1/ROS/SNAIL axis is a key subset of the crosstalk. When these crosstalks are active, our current model suggests metabolic reprogramming drives EMT. However, our model is also consistent with previous work that suggests EMT can drive metabolic reprogramming [29,83,84]. As we've noted, studying these networks in isolation is just the first step in understanding how metastasis is driven by these networks, and incorporating additional networks will be necessary to fully answer this question. For instance, previous

studies coupling EMT, stemness, and Notch signaling have shown the various phenotypes associated with therapy resistance, increased metastatic potential, and stem-like properties tend to be correlated [85–87]. However, these couplings also resulted in unexpected behaviors such as the co-localization of hybrid E/M cells [85] and a stemness window that was tunable [86]. Consequently, studying individual gene regulatory network modules, even in the presence of signals, is unable to give a thorough understanding of the network properties. Therefore, to understand how the various phenotypes are correlated, and potentially identify key regulators, multiple networks and crosstalks should be studied concurrently. One potential coupling would be the EMT network, stemness network, metabolic network, Notch-Jagged signaling, KEAP/NRF2 pathway, and the immune-suppressor PD-L1 (Fig. S?). From this expansive network, we expect therapy resistance, increased metastatic potential, increased invasiveness, hybrid metabolism phenotypes, immune-evasive properties, and stem-like properties to be correlated and key regulators could be identified.

Acknowledgements

This work was supported by National Science Foundation by sponsoring the Center for Theoretical Biological Physics – award PHY-2019745 (JNO, HL) and by awards PHY-1605817 (HL), CHE-1614101 (JNO), and PHY-1522550 (JNO, MG). JNO is a CPRIT Scholar in Cancer Research. MG was also supported by the NSF GRFP no. 1842494.

References

1. Hanahan D. Hallmarks of Cancer: New Dimensions. Cancer Discov. 2022;12(1):31–46.

2. Kalluri R. EMT: When epithelial cells decide to become mesenchymal-like cells. J Clin Invest. 2009;119(6):1417–9.

3. Hay ED. The mesenchymal cell, its role in the embryo, and the remarkable signaling mechanisms that create it. Dev Dynam. 2005;233(3):706–20.

4. Pietilä M, Ivaska J, Mani SA. Whom to blame for metastasis, the epithelial–mesenchymal transition or the tumor microenvironment? Cancer Lett. 2016;380(1):359–68.

5. Talbot LJ, Bhattacharya SD, Kuo PC. Epithelial-mesenchymal transition, the tumor microenvironment, and metastatic behavior of epithelial malignancies. Int J Biochem Mol Biol. 2012 May 18;3(2):117–36.

6. Cho ES, Kang HE, Kim NH, Yook JI. Therapeutic implications of cancer epithelial-mesenchymal transition (EMT). Arch Pharm Res. 2019;42(1):14–24.

7. Lu M, Jolly MK, Levine H, Onuchic JN, Ben-Jacob E. MicroRNA-based regulation of epithelial–hybrid–mesenchymal fate determination. Proc National Acad Sci. 2013;110(45):18144–9.

8. Saitoh M. Involvement of partial EMT in cancer progression. J Biochem. 2018;164(4):257–64.

9. Saxena K, Jolly MK, Balamurugan K. Hypoxia, partial EMT and collective migration: Emerging culprits in metastasis. Transl Oncol. 2020;13(11):100845.

10. Bakir B, Chiarella AM, Pitarresi JR, Rustgi AK. EMT, MET, Plasticity, and Tumor Metastasis. Trends Cell Biol. 2020;30(10):764–76.

11. Pastushenko I, Blanpain C. EMT Transition States during Tumor Progression and Metastasis. Trends Cell Biol. 2018;29(3):212–26.

12. Fustaino V, Presutti D, Colombo T, Cardinali B, Papoff G, Brandi R, et al. Characterization of epithelial-mesenchymal transition intermediate/hybrid phenotypes associated to resistance to EGFR inhibitors in non-small cell lung cancer cell lines. Oncotarget. 2017;8(61):103340–63.

13. George JT, Jolly MK, Xu J, Somarelli J, Levine H. Survival outcomes in cancer patients predicted by a partial EMT gene expression scoring metric. Cancer Res. 2017;77(22):canres.3521.2016.

14. Jolly MK, Tripathi SC, Jia D, Mooney SM, Celiktas M, Hanash SM, et al. Stability of the hybrid epithelial/mesenchymal phenotype. Oncotarget. 2016;7(19):27067–84.

15. Pastushenko I, Brisebarre A, Sifrim A, Fioramonti M, Revenco T, Boumahdi S, et al. Identification of the tumour transition states occurring during EMT. Nature. 2018;556(7702):463–8.

16. Simeonov KP, Byrns CN, Clark ML, Norgard RJ, Martin B, Stanger BZ, et al. Single-cell lineage tracing of metastatic cancer reveals selection of hybrid EMT states. Cancer Cell. 2021;39(8):1150-1162.e9.

17. Dey P, Kimmelman AC, DePinho RA. Metabolic Codependencies in the Tumor Microenvironment. Cancer Discov. 2021;candisc.1211.2020.

18. Warburg O, Wind F, Negelein E. THE METABOLISM OF TUMORS IN THE BODY. J Gen Physiol. 1927;8(6):519–30.

19. Liberti MV, Locasale JW. The Warburg Effect: How Does it Benefit Cancer Cells? Trends Biochem Sci. 2016;41(3):211–8.

20. Ohshima K, Morii E. Metabolic Reprogramming of Cancer Cells during Tumor Progression and Metastasis. Metabolites. 2021;11(1):28.

21. Carvalho TMA, Cardoso HJ, Figueira MI, Vaz CV, Socorro S. The peculiarities of cancer cell metabolism: A route to metastasization and a target for therapy. Eur J Med Chem. 2019;171:343–63.

22. Nagao A, Kobayashi M, Koyasu S, Chow CCT, Harada H. HIF-1-Dependent Reprogramming of Glucose Metabolic Pathway of Cancer Cells and Its Therapeutic Significance. Int J Mol Sci. 2019;20(2):238.

23. Cheng Y, Lu Y, Zhang D, Lian S, Liang H, Ye Y, et al. Metastatic cancer cells compensate for low energy supplies in hostile microenvironments with bioenergetic adaptation and metabolic reprogramming. Int J Oncol. 2018;53(6):2590–604.

24. Porporato PE, Payen VL, Pérez-Escuredo J, De Saedeleer CJ, Danhier P, Copetti T, et al. A Mitochondrial Switch Promotes Tumor Metastasis. Cell Reports. 2014;8(3):754–66.

25. Jia D, Park JH, Jung KH, Levine H, Kaipparettu BA. Elucidating the Metabolic Plasticity of Cancer: Mitochondrial Reprogramming and Hybrid Metabolic States. Cells. 2018;7(3):21.

26. Jia D, Paudel BB, Hayford CE, Hardeman KN, Levine H, Onuchic JN, et al. Drug-Tolerant Idling Melanoma Cells Exhibit Theory-Predicted Metabolic Low-Low Phenotype. Frontiers Oncol. 2020;10:1426.

27. Dupuy F, Tabariès S, Andrzejewski S, Dong Z, Blagih J, Annis MG, et al. PDK1-Dependent Metabolic Reprogramming Dictates Metastatic Potential in Breast Cancer. Cell Metab. 2015;22(4):577–89.

28. LeBleu VS, O'Connell JT, Herrera KNG, Wikman H, Pantel K, Haigis MC, et al. PGC-1α mediates mitochondrial biogenesis and oxidative phosphorylation in cancer cells to promote metastasis. Nat Cell Biol. 2014;16(10):992–1003.

29. Jia D, Park JH, Kaur H, Jung KH, Yang S, Tripathi S, et al. Towards decoding the coupled decision-making of metabolism and epithelial-to-mesenchymal transition in cancer. Brit J Cancer. 2021;1–10.

30. Serocki M, Bartoszewska S, Janaszak-Jasiecka A, Ochocka RJ, Collawn JF, Bartoszewski R. miRNAs regulate the HIF switch during hypoxia: a novel therapeutic target. Angiogenesis. 2018;21(2):183–202.

31. Shang Y, Chen H, Ye J, Wei X, Liu S, Wang R. HIF-1α/Ascl2/miR-200b regulatory feedback circuit modulated the epithelial-mesenchymal transition (EMT) in colorectal cancer cells. Exp Cell Res. 2017;360(2):243–56.

32. Jin HF, Wang JF, Song TT, Zhang J, Wang L. MiR-200b Inhibits Tumor Growth and Chemoresistance via Targeting p70S6K1 in Lung Cancer. Frontiers Oncol. 2020;10:643.

33. Georgakopoulos-Soares I, Chartoumpekis DV, Kyriazopoulou V, Zaravinos A. EMT Factors and Metabolic Pathways in Cancer. Frontiers Oncol. 2020;10:499.

34. Fedele M, Sgarra R, Battista S, Cerchia L, Manfioletti G. The Epithelial–Mesenchymal Transition at the Crossroads between Metabolism and Tumor Progression. Int J Mol Sci. 2022;23(2):800.

35. Burger GA, Danen EHJ, Beltman JB. Deciphering Epithelial–Mesenchymal Transition Regulatory Networks in Cancer through Computational Approaches. Frontiers Oncol. 2017;7:162.

36. Hu Y, Xu W, Zeng H, He Z, Lu X, Zuo D, et al. OXPHOS-dependent metabolic reprogramming prompts metastatic potential of breast cancer cells under osteogenic differentiation. Brit J Cancer. 2020;123(11):1644–55.

37. Sung JY, Cheong JH. Pan-Cancer Analysis Reveals Distinct Metabolic Reprogramming in Different Epithelial–Mesenchymal Transition Activity States. Cancers. 2021;13(8):1778.

38. Choudhary KS, Rohatgi N, Halldorsson S, Briem E, Gudjonsson T, Gudmundsson S, et al. EGFR Signal-Network Reconstruction Demonstrates Metabolic Crosstalk in EMT. Plos Comput Biol. 2016;12(6):e1004924.

39. Feng S, Zhang L, Liu X, Li G, Zhang B, Wang Z, et al. Low levels of AMPK promote epithelial-mesenchymal transition in lung cancer primarily through HDAC4- and HDAC5-mediated metabolic reprogramming. J Cell Mol Med. 2020;24(14):7789–801.

40. Kang X, Wang J, Li C. Exposing the Underlying Relationship of Cancer Metastasis to Metabolism and Epithelial-Mesenchymal Transitions. Iscience. 2019;21:754–72.

41. Kang X, Li C. A Dimension Reduction Approach for Energy Landscape: Identifying Intermediate States in Metabolism-EMT Network. Adv Sci. 2021;2003133.

42. Sciacovelli M, Frezza C. Metabolic reprogramming and epithelial-to-mesenchymal transition in cancer. Febs J. 2017;284(19):3132–44.

43. Huang R, Zong X. Aberrant cancer metabolism in epithelial–mesenchymal transition and cancer metastasis: Mechanisms in cancer progression. Crit Rev Oncol Hemat. 2017;115:13–22.

44. Jiang L, Xiao L, Sugiura H, Huang X, Ali A, Kuro-o M, et al. Metabolic reprogramming during TGFβ1-induced epithelial-to-mesenchymal transition. Oncogene. 2015;34(30):3908–16.

45. Bocci F, Tripathi SC, Mercedes SAV, George JT, Casabar JP, Wong PK, et al. NRF2 activates a partial epithelial-mesenchymal transition and is maximally present in a hybrid epithelial/mesenchymal phenotype. Integr Biol. 2019;11(6):251–63.

46. Luo M, Shang L, Brooks MD, Jiagge E, Zhu Y, Buschhaus JM, et al. Targeting Breast Cancer Stem Cell State Equilibrium through Modulation of Redox Signaling. Cell Metab. 2018;28(1):69-86.e6.

47. Colacino JA, Azizi E, Brooks MD, Harouaka R, Fouladdel S, McDermott SP, et al. Heterogeneity of Human Breast Stem and Progenitor Cells as Revealed by Transcriptional Profiling. Stem Cell Rep. 2018;10(5):1596–609.

48. Yu L, Lu M, Jia D, Ma J, Ben-Jacob E, Levine H, et al. Modeling the Genetic Regulation of Cancer Metabolism: Interplay between Glycolysis and Oxidative Phosphorylation. Cancer Res. 2017;77(7):1564–74.

49. Jia D, Li X, Bocci F, Tripathi S, Deng Y, Jolly MK, et al. Quantifying Cancer Epithelial-Mesenchymal Plasticity and its Association with Stemness and Immune Response. J Clin Medicine. 2019;8(5):725.

50. Lu M, Jolly MK, Gomoto R, Huang B, Onuchic J, Ben-Jacob E. Tristability in Cancer-Associated MicroRNA-TF Chimera Toggle Switch. J Phys Chem B. 2013;117(42):13164–74.

51. Kovac S, Angelova PR, Holmström KM, Zhang Y, Dinkova-Kostova AT, Abramov AY. Nrf2 regulates ROS production by mitochondria and NADPH oxidase. Biochimica Et Biophysica Acta Bba - Gen Subj. 2015;1850(4):794–801.

52. He F, Ru X, Wen T. NRF2, a Transcription Factor for Stress Response and Beyond. Int J Mol Sci. 2020;21(13):4777.

53. Li N, Muthusamy S, Liang R, Sarojini H, Wang E. Increased expression of miR-34a and miR-93 in rat liver during aging, and their impact on the expression of Mgst1 and Sirt1. Mech Ageing Dev. 2011;132(3):75–85.

54. Bai XY, Ma Y, Ding R, Fu B, Shi S, Chen XM. miR-335 and miR-34a Promote Renal Senescence by Suppressing Mitochondrial Antioxidative Enzymes. J Am Soc Nephrol. 2011;22(7):1252–61.

55. Navarro F, Lieberman J. miR-34 and p53: New Insights into a Complex Functional Relationship. Plos One. 2015;10(7):e0132767.

56. Italiano D, Lena AM, Melino G, Candi E. Identification of NCF2/p67phox as a novel p53 target gene. Cell Cycle. 2012;11(24):4589–96.

57. Chou HL, Fong Y, Wei CK, Tsai EM, Chen JYF, Chang WT, et al. A Quinone-Containing Compound Enhances Camptothecin-Induced Apoptosis of Lung Cancer Through Modulating Endogenous ROS and ERK Signaling. Arch Immunol Ther Ex. 2017;65(3):241–52.

58. Byun Y, Choi YC, Jeong Y, Lee G, Yoon S, Jeong Y, et al. MiR-200c downregulates HIF-1α and inhibits migration of lung cancer cells. Cell Mol Biol Lett. 2019;24(1):28.

59. Bartoszewska S, Rochan K, Piotrowski A, Kamysz W, Ochocka RJ, Collawn JF, et al. The hypoxia-inducible miR-429 regulates hypoxia-inducible factor-1α expression in human endothelial cells through a negative feedback loop. Faseb J. 2015;29(4):1467–79.

60. Xu X, Tan X, Tampe B, Sanchez E, Zeisberg M, Zeisberg EM. Snail Is a Direct Target of Hypoxia-inducible Factor 1α (HIF1α) in Hypoxia-induced Endothelial to Mesenchymal Transition of Human Coronary Endothelial Cells*. J Biol Chem. 2015;290(27):16653–64.

61. Chou CC, Lee KH, Lai IL, Wang D, Mo X, Kulp SK, et al. AMPK Reverses the Mesenchymal Phenotype of Cancer Cells by Targeting the Akt–MDM2–Foxo3a Signaling Axis. Cancer Res. 2014;74(17):4783–95.

62. Ohshima J, Wang Q, Fitzsimonds ZR, Miller DP, Sztukowska MN, Jung YJ, et al. Streptococcus gordonii programs epithelial cells to resist ZEB2 induction by Porphyromonas gingivalis. Proc National Acad Sci. 2019;116(17):201900101.

63. Dong T, Zhang Y, Chen Y, Liu P, An T, Zhang J, et al. FOXO1 inhibits the invasion and metastasis of hepatocellular carcinoma by reversing ZEB2-induced epithelial-mesenchymal transition. Oncotarget. 2016;8(1):1703–13.

64. Huang W, Cao J, Liu X, Meng F, Li M, Chen B, et al. AMPK Plays a Dual Role in Regulation of CREB/BDNF Pathway in Mouse Primary Hippocampal Cells. J Mol Neurosci. 2015;56(4):782–8.

65. Jin H, Xue L, Mo L, Zhang D, Guo X, Xu J, et al. Downregulation of miR-200c stabilizes XIAP mRNA and contributes to invasion and lung metastasis of bladder cancer. Cell Adhes Migr. 2019;13(1):236–48.

66. Janin M, Esteller M. Oncometabolite Accumulation and Epithelial-to-Mesenchymal Transition: The Turn of Fumarate. Cell Metab. 2016;24(4):529–30.

67. Zhang Q, Zheng S, Wang S, Wang W, Xing H, Xu S. Chlorpyrifos induced oxidative stress to promote apoptosis and autophagy through the regulation of miR-19a-AMPK axis in common carp. Fish Shellfish Immun. 2019;93:1093–9.

68. Thomson DM, Herway ST, Fillmore N, Kim H, Brown JD, Barrow JR, et al. AMP-activated protein kinase phosphorylates transcription factors of the CREB family. J Appl Physiol. 2008;104(2):429–38.

69. Muralidharan S, Sahoo S, Saha A, Chandran S, Majumdar SS, Mandal S, et al. Quantifying the Patterns of Metabolic Plasticity and Heterogeneity along the Epithelial–Hybrid–Mesenchymal Spectrum in Cancer. Biomol. 2022;12(2):297.

70. Tripathi S, Kessler DA, Levine H. Biological Networks Regulating Cell Fate Choice Are Minimally Frustrated. Phys Rev Lett. 2020;125(8):088101.

71. Farris JC, Pifer PM, Zheng L, Gottlieb E, Denvir J, Frisch SM. Grainyhead-like 2 Reverses the Metabolic Changes Induced by the Oncogenic Epithelial–Mesenchymal Transition: Effects on Anoikis. Mol Cancer Res. 2016;14(6):528–38.

72. Radisky DC, Levy DD, Littlepage LE, Liu H, Nelson CM, Fata JE, et al. Rac1b and reactive oxygen species mediate MMP-3-induced EMT and genomic instability. Nature. 2005;436(7047):123–7.

73. Mori K, Uchida T, Yoshie T, Mizote Y, Ishikawa F, Katsuyama M, et al. A mitochondrial ROS pathway controls matrix metalloproteinase 9 levels and invasive properties in RAS-activated cancer cells. Febs J. 2019;286(3):459–78.

74. Ishikawa K, Takenaga K, Akimoto M, Koshikawa N, Yamaguchi A, Imanishi H, et al. ROS-Generating Mitochondrial DNA Mutations Can Regulate Tumor Cell Metastasis. Science. 2008;320(5876):661–4.

75. SHIDA M, KITAJIMA Y, NAKAMURA J, YANAGIHARA K, BABA K, WAKIYAMA K, et al. Impaired mitophagy activates mtROS/HIF-1α interplay and increases cancer aggressiveness in gastric cancer cells under hypoxia. Int J Oncol. 2016;48(4):1379–90.

76. Babaei G, Raei N, milani AT, Aziz SGG, Pourjabbar N, Geravand F. The emerging role of miR-200 family in metastasis: focus on EMT, CSCs, angiogenesis, and anoikis. Mol Biol Rep. 2021;48(10):6935–47.

77. Tripathi S, Park JH, Pudakalakatti S, Bhattacharya PK, Kaipparettu BA, Levine H. A mechanistic modeling framework reveals the key principles underlying tumor metabolism. Plos Comput Biol. 2022;18(2):e1009841.

78. Thiery JP, Acloque H, Huang RYJ, Nieto MA. Epithelial-Mesenchymal Transitions in Development and Disease. Cell. 2009;139(5):871–90.

79. Zhang K, Zhaos J, Liu X, Yan B, Chen D, Gao Y, et al. Activation of NF-B upregulates Snail and consequent repression of E-cadherin in cholangiocarcinoma cell invasion. Hepato-gastroenterol. 2011;58(105):1–7.

80. Jia D, Lu M, Jung KH, Park JH, Yu L, Onuchic JN, et al. Elucidating cancer metabolic plasticity by coupling gene regulation with metabolic pathways. Proc National Acad Sci. 2019;116(9):201816391.

81. Graziani V, Rodriguez-Hernandez I, Maiques O, Sanz-Moreno V. The amoeboid state as part of the epithelial-to-mesenchymal transition programme. Trends Cell Biol. 2021;32(3):228–42.

82. Sanz-Moreno V, Crosas-Molist ECM, Maiques O, Graziani V, Pandya P, Monger J, et al. AMPK is a mechano-metabolic sensor linking cell adhesion and mitochondrial dynamics to Myosin II dependent cell migration. 2022;

83. Miyazono K. Transforming growth factor-β signaling in epithelial-mesenchymal transition and progression of cancer. Proc Jpn Acad Ser B Phys Biological Sci. 2009;85(8):314–23.

84. Zhang J, Tian XJ, Xing J. Signal Transduction Pathways of EMT Induced by TGF-β, SHH, and WNT and Their Crosstalks. J Clin Medicine. 2016;5(4):41.

85. Bocci F, Gearhart-Serna L, Boareto M, Ribeiro M, Ben-Jacob E, Devi GR, et al. Toward understanding cancer stem cell heterogeneity in the tumor microenvironment. Proc National Acad Sci. 2018;116(1):201815345.

86. Jolly MK, Jia D, Boareto M, Mani SA, Pienta KJ, Ben-Jacob E, et al. Coupling the modules of EMT and stemness: A tunable ‘stemness window’ model. Oncotarget. 2015;6(28):25161–74.

87. Bocci F, Jolly MK, George JT, Levine H, Onuchic JN. A mechanism-based computational model to capture the interconnections among epithelial-mesenchymal transition, cancer stem cells and Notch-Jagged signaling. Oncotarget. 2018;9(52):29906–20.